Geminate and distant-pair radiative recombination in porous silicon

1999 J. Phys.: Condens. Matter 11 4783

(http://iopscience.iop.org/0953-8984/11/24/318)

J. Phys.: Condens. Matter **11** (1999) 4783–4800. Printed in the UK PII: S0953-8984(99)00842-5

Geminate and distant-pair radiative recombination in porous silicon

N P Kovalenko†§, I K Doycho†, S A Gevelyuk†, V A Vorobyeva† and Ya O Roizin‡

† State University, 270026 Odessa, Ukraine
‡ Tower Semiconductor Limited, PO Box 619, Migdal Haemek, 23105, Israel

E-mail: npk@paco.net

Received 6 January 1999, in final form 7 April 1999

Abstract. We have performed time-resolved measurements of porous silicon (PS) photoluminescence (PL) at temperatures in the range from 15 K to 300 K for different emission energies. For the first time we have observed lifetimes of radiative recombination ranging from nanoseconds to seconds. Strong phosphorescence was revealed for as-prepared samples at 15 K and also for partly oxidized specimens at room temperature. The PS luminescence had a polarized component that was strongly dependent upon the detection energy and the prehistory of the specimens studied. We analyse two possible scenarios of radiative recombination in PS: (1) migration of non-equilibrium charge carriers between nanometre-sized silicon clusters prior to recombination; (2) geminate recombination of charge carriers thermalized in the same or neighbouring silicon domains. Combination of these scenarios allows us to explain the PL of PS on all timescales from one viewpoint. We present direct Monte Carlo simulations of recombination processes in PS, and show that the results are in good agreement with experimental data.

1. Introduction

The luminescence of porous silicon (PS) fabricated by electrochemical anodization of crystalline silicon has been extensively studied in recent years. Nevertheless, to date, our understanding of light emission from PS remains incomplete. Two principal models that explain the photoluminescence (PL) are generally recognized. The PL was attributed by Canham [1, 2] to quantum confinement of excitons in Si clusters of nanometre sizes. A lot of further research performed by different authors confirmed the quantum-confinement idea [3–6]. On the other hand, with the large surface-to-volume ratio for the highly porous structure, surface states (surface species) at the surfaces of silicon nanocrystallites could plausibly act as luminescent centres [7–9]. Various kinds of study have been made including ODMR studies, Raman spectroscopy, electron and tunnelling microscopy, and various luminescence measurements [10–12], to distinguish between the quantum-confinement and surface models for PS samples. The main argument for the quantum-confinement model is the dependence of the PL spectra on the sizes of silicon clusters in PS. In particular, it is possible to explain the blue-shift of the PL in partly oxidized specimens by the decrease of Si cluster sizes. The main arguments for the surface model are the changes of PL efficiency caused by various treatments of PS with

§ Author to whom any correspondence should be addressed. Mailing address: Odessa State University, 2 Dvoryanskaya Street, 270026 Odessa, Ukraine. Telephone and fax: +38(0482)238936.

0953-8984/99/244783+18$19.50

different mild chemicals. There has been much controversy over most aspects of both models, and many authors introduced further models to explain various details of the experimental behaviour of the PL. These models incorporate both nanostructures for quantum confinement and luminescent centres at the surfaces or between the silicon clusters [13–15]. For luminescent centres in the 'hybrid' model, the radiation absorbed in PS creates electron–hole pairs in Si clusters, but the non-equilibrium pairs can diffuse out and recombine at the luminescent centres.

Most of the models mentioned encounter serious difficulties in explaining certain features, as in most surface models they are attributed to compounds of silicon with oxygen and hydrogen, amorphous silicon phases, etc [16, 17]. According to the wide range of time constants encountered in radiative recombination processes in PS [10], PL lifetimes range from picoseconds to milliseconds. We have shown in this paper that this range should be extended up to seconds. The typical bell-shaped PL spectra of porous silicon fabricated under various experimental conditions and the changes that these spectra undergo during oxidation are also puzzling [18]. To explain the spectral dependencies, most authors utilize peaked size distributions of quantum clusters [19], though these distributions are not always consistent with microstructure observations. Moreover, several PL mechanisms are generally taken into account to explain the emission properties over the wide spectral range and for different lifetimes. Most of the models discussed consider radiative recombination as a geminate process (an electron recombines with the hole created in the same cluster). The alternative is that electrons and holes created by excitation light intermix before recombination [20]. In the latter case, diffusion of charge carriers can take place before the radiative recombination of distant pairs, in a similar way to what happens in disordered semiconductors [21, 22].

In this paper we propose a new approach to the problem of PL in porous silicon. Our time-resolved PL measurements over a wide temperature range as well as spectral and polarization measurements for as-fabricated and oxidized PS strongly imply that the energy transfer associated with migration of electrons and holes between quantum-sized crystallites must be taken into account. The band edges of these crystallites depend on their sizes. Together with traps in the intercluster regions, crystallites form a staircase of energy states for downward hopping. The idea is similar to the one proposed in [23] in the sense that our approach also employs downward hopping of electrons and holes before recombination. Nevertheless, it differs fundamentally because it accounts for hops of carriers in the tails of localized states and does not include excitation over the mobility edge. To verify these qualitative ideas, we have performed a direct Monte Carlo simulation of PS structure and a subsequent simulation of the distant-pair radiative recombination that takes place after the end of the excitation light pulse. The results obtained give an internally coherent picture of PS light emission. The proposed model accounts for much of the experimental behaviour of the PL. In particular, the results of our calculations are shown to be in good agreement with experimental recombination kinetics and light emission spectra. There is strong evidence that energy migration processes dominate the recombination kinetics even at temperatures as low as 15 K. We would like to mention that the approach used in our modelling differs from existing Monte Carlo simulations [24], where out-diffusion of excitons is supposed. In our case we consider independent hops of holes and electrons after their random thermalization. Moreover, we model both the spatial structure of PS and the charge-carrier recombination kinetics.

The organization of this paper is as follows. In section 2 we give a brief review of the physical models that have been put forward to explain the PL decay kinetics after pulsed excitation, and analyse their physical limitations. Our model is also discussed in this section, and the results of computer simulation are presented. In section 3 we analyse original experimental data relevant to the model, and finally in section 4 we show how the proposed model accounts for much of the experimental behaviour of PL in porous silicon.

2. Simulation of recombination processes in porous silicon

2.1. Existing models

A great number of time-resolved PL measurements have already been reported for a wide range of lifetimes τ_e from picoseconds to milliseconds [17]. The possible models that can, in principal, explain the lifetimes exceeding tens of microseconds can be divided into three groups:

(a) size-dependent radiative lifetimes of excitons in quantum wells of PS [25, 26];
(b) tunnelling of photoexcited charge carriers between silicon crystallites where radiative recombination occurs [27, 28];
(c) radiative recombination through metastable states dispersed in energy and space, and located at the surface or in the vicinity of silicon particles [29–31].

In the first case the lifetimes spreading from nanoseconds to milliseconds are explained by different values of momentum matrix elements for electronic transitions for Si domains with different confinement sizes. If the corresponding time constants are considered as radiative lifetimes t, these values correspond to quantum dot diameters ranging from 1 nm to 3 nm. The confinement size should be as small as a few times the lattice constant to account for time constants of the order of those observed for direct-gap semiconductors. At the same time, lifetimes exceeding seconds are predicted by this model for a quantum dot radius of the order of 3 nm [25]. Unfortunately, these estimates of quantum dot sizes are not self-consistent with those obtained from luminescence peak energies. The latter give larger sizes of quantum dots. These discrepancies are reconciled by the authors of [25, 32] by introducing non-radiative recombination processes due to dangling bonds at Si crystallite surfaces. In particular, diminution of the carrier localization length was analysed in [32] as a factor modulating the probability of reaching non-radiative centres for oxidized PS and at increased temperatures. It is important to note that when the rate of non-radiative recombination decreases with the temperature decrease, we should have a pronounced increase of the PL intensity at low temperatures. An increase of t of the same order of magnitude must also be observed. As follows from the results of section 3, the situation in our case was quite different.

The second possible explanation of τ_e spreading over ten decades is tunnelling. This process can be radiative or non-radiative. If the electron and hole are spatially separated, the radiative tunnelling probability can determine the PL lifetime. If we consider small overlap of the electron and hole wave functions, the corresponding pair can remain in the excited state for a rather long time before radiative recombination. In this case, charge carriers can also escape to other regions where they recombine non-radiatively. In particular, a model that takes for the non-radiative process a tunnelling and a thermally activated escape of the photoexcited carriers through barriers with a Gaussian distribution in height explains the non-exponential PL decay and the wide range of lifetimes [27]. This model encounters the same difficulties in interpreting the thermal dependencies as the exciton models. Moreover, non-radiative tunnelling [28] alone cannot explain the PL kinetics in dry-oxidized PS specimens [18]. The increase in the SiO_2 barriers between Si clusters was expected to lead to the increase of luminescence lifetimes in PS. If the lifetimes were connected with radiative tunnelling, oxidation should result in the decrease of PL intensity. Contrary to both assumptions, the PL intensity increased while τ_e did not change significantly. It should be noted that other authors [29] report a decrease of PL intensity and radiative lifetimes resulting from oxidation. Similar results were obtained in our measurements (see section 3). We definitely encounter differences in properties for samples of PS fabricated in different laboratories.

The third group of models relates the PL to radiative recombination via localized states at Si crystallite surfaces or, in the non-stoichiometric compound, between Si domains. The existence of long-living metastable states is generally postulated. Large time constants can be related to configurational changes in the chemical complexes responsible for traps. A number of candidates were discussed in the literature, in particular NBOHC (the non-bridging oxygen hole centre) [30], etc. Corresponding numerical models [31] include too many parameters to be directly compared with experimental data. It is also difficult to interpret changes of lifetimes occurring as a result of oxidation. Moreover, in contrast with the previous two models where recombination occurs in Si nanocrystallites, the last group of models encounters significant difficulties in explaining the large degree of PS luminescence polarization (see section 4).

Taking into account the fact that PS samples are prepared in very different ways, any of the above-mentioned mechanisms can, in principal, be appropriate in certain conditions. The problem is that of establishing which of them accounts for much of the experimental behaviour of a certain sample of PS, with the minimum number of assumptions. We were unable to explain the known experimental results and those obtained in this work using the above-reviewed models. In this study we have developed a modified version of the tunnelling model. We analyse the processes of charge-carrier thermalization in silicon crystallites and their subsequent diffusion between quantum-sized domains prior to radiative recombination. We simulate both the structure of light-emitting PS and the behaviour of the non-equilibrium charge carriers.

2.2. Spatial and band structure of radiative PS

We visualize luminescent PS as a gel-like material on the walls of micrometre-sized cavities. In figure 1 SEM photographs are presented that show the surface of the silicon substrate after our PS was mechanically detached. The image (a) was obtained in a standard observation regime while image (b) was taken in the regime of luminescence registration. This allows us to visualize the gel-like region on the surfaces of micrometre-sized voids, and to conclude that the PL originates from this microporous gel. Similar results were reported by other authors

(a)

(b)

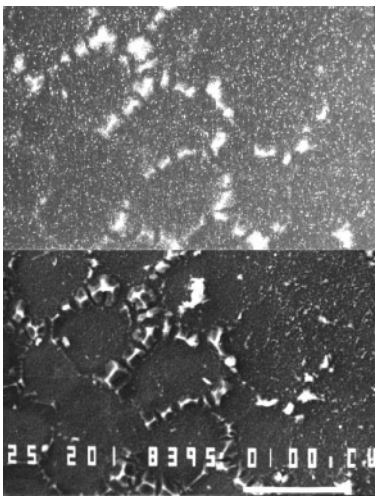

Figure 1. Spatial structure of PS. The surface of the silicon substrate after the PS film has been mechanically detached: (a) a standard SEM image; (b) an image taken in the luminescent regime.

[33]. The x-ray microprobe analysis shows that even our initial (non-oxidized) PS incorporates a large amount of oxygen (up to 30 mol%; for details of the technology see section 3). It consists of quantum-sized silicon crystallites surrounded by voids and SiO_x:H fragments. Porosity measurements (weighing of free-standing films) have shown that the integral porosity of our specimens exceeds 70–80%. We assign this value also to the luminescent gel-like region of our PS.

Porous silicon can be considered as a typical disordered system. Inhomogeneous potential relief is inherent to PS due to variations in the sizes of silicon domains that result in variations of the effective band-gap energies E_r, where E_r is the band-gap of a cluster having radius r. The shapes of the quantum-sized domains are rather complicated. A reasonable approximation that allows us to perform calculations is that of taking the silicon crystallites to have spherical form. These crystallites can contact or intersect to a certain extent, forming clusters consisting of spheres. The radiative recombination in our model is supposed to occur in quantum-sized crystallites. Their size is directly connected with the emission energy. Following [34], an implicit relation between the emission wavelength and the radius of the sphere r can be written as follows:

$$\lambda = \frac{2\pi\hbar c}{E_{\mathrm{Si}} + \Delta E_1 + \Delta E_2} \qquad \Delta E_{1,2} = \frac{\hbar^2 k^2}{2m_{n,p}} \tag{1}$$

where k is the solution of the equation

$$\sin(kr) = \pm kr\sqrt{\frac{\hbar^2}{2m_{n,p}r^2U_0}} \qquad \mathrm{cotan}(kr) < 0 \qquad \text{(the level with } \lambda = 0\text{)}. \tag{2}$$

m_n and m_p are the effective masses of the electrons and holes confined in the silicon crystallites, respectively; U_0 is the potential barrier at the surface of the cluster (about 4–5 eV). The results of these simple estimations are in good agreement with the $\lambda(r)$ dependencies obtained by cluster and quantum wire calculations [35, 36].

We avoid certain assumptions concerning the structure of the media interconnecting Si clusters. We argue that it is a kind of a complicated non-stoichiometric silicon–oxygen–hydrogen porous compound incorporating a large number of traps both for electrons and holes (e.g., on the surfaces of the porous SiO_x:H). Modification of the intercrystallite medium results in variations in the position of the PS mobility edges. In particular, charge transport between Si crystallites can be suppressed if this medium is substituted for high-quality silicon dioxide.

We have performed a Monte Carlo simulation of PS structure in the following way. A set of spheres were taken with the radii ranging from 1 nm to 1.5 nm with a Gaussian size distribution ($r < r_{min}$). The parameters of this distribution were the only fitting parameters in our simulation of PS structure. Spheres of different sizes were randomly placed in space to obtain the experimental value of the PS porosity (∼80%). The side of the cube intended for realization of the radiation recombination scenario was about 5 nm. 150 different spatial configurations were generated to simulate the recombination processes. The results of the simulation were averaged over these configurations. Figure 2 shows a schematic band diagram of the system studied. The regions of the Si domains are separated by energy barriers consisting of microporous SiO_2 (non-stoichiometric, and containing large amounts of hydrogen). Electrons and holes can tunnel through these barriers prior to recombination. The typical tunnelling length for electrons is

$$\alpha = \sqrt{2\hbar^2 m_n \Phi_0}$$

which is of the order of 0.1 nm in this case ($\Phi = \Phi_0 - \Delta E$; $\Phi_0 \sim 3.1$ eV for the barrier at the crystalline Si–SiO_2 interface). It is clear that there may be some additional charge-transport

paths between silicon crystallites. A probable candidate is a hopping path via localized states at the surfaces of microvoids in SiO_x:H. The parameters of this path should be extremely sensitive to the preparation conditions, subsequent treatments, handling, and aging.

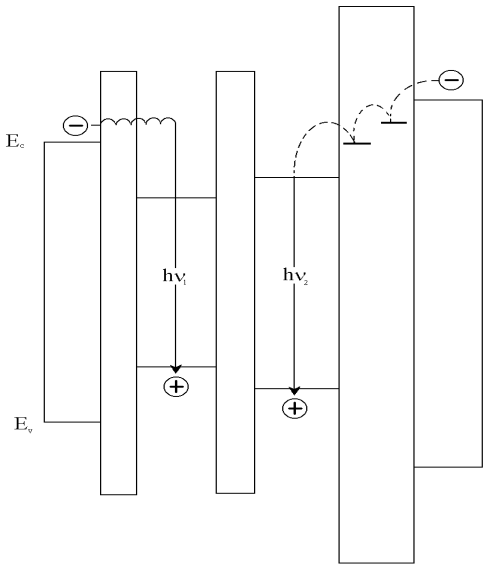

Figure 2. A schematic energy diagram of PS consisting of quantum crystallites that have various band-gaps. Transitions of electrons and holes between crystallites prior to recombination are shown by arrows (solid lines: tunnelling; dashed curves: hopping via localized states).

2.3. Recombination kinetics

Little is known about the excited charge-carrier thermalization process in porous silicon. In the experiments a large density of electron–hole pairs was generated by a nanosecond laser pulse (10^{20}–10^{21} cm^{-3}). The energy of the excitation quanta was about $E_e = 3.7$ eV (with a nitrogen pulsed laser). We consider that the initial stage of the thermalization process is similar to that commonly accepted to occur in amorphous silicon [37]. The charge carriers thermalize rapidly to the band edges of individual crystallites in PS. In this process they can diffuse some distance apart, which will depend upon the energy of the excitation quanta, the energy gap of the crystallite at the position where they are excited, and the energy of the PS mobility edges (E_{me} for electrons). The mean energy that is dissipated before the carrier is at the mobility edge $\bar{E}$ for PS is

$$\Delta E = h\nu - E_{gi}/2 - \bar{E}$$

where $h\nu$ is the energy of the excitation quanta and E_{gi} is the band-gap of the $r = r_i$ crystallites. We consider that the most efficient channel of energy relaxation is excitation of local phonons at the surfaces of silicon nanocrystallites. The characteristic phonon energy E_p in this case is about 0.1 eV. This energy corresponds to oscillations of S–H and Si–O–Si complexes that were most pronounced in the IR absorption spectra of our specimens (analogous data were obtained for similar samples in [29]). A simple estimate based on the indeterminacy relation

gives for the minimum diffusion length L_d

$$L_d = \frac{\sqrt{\hbar\,\Delta E\,D}}{E_p}. \tag{3}$$

Taking a diffusion coefficient typical for disordered semiconductors, of the order of $D = 1\ \mathrm{cm}^2\ \mathrm{s}^{-1}$, and $\Delta E = 1$ eV, we get diffusion lengths exceeding 2.5 nm in the rapid-thermalization process lasting $\tau_1 > \hbar\,\Delta E/E_p^2 \sim 5 \times 10^{-14}$ s. It should be noted that we have supposed that non-equilibrium electrons and holes at the mobility edge lose the remaining excess energy in corresponding single-potential wells (crystallites). If the diffusion process continues for energies below $\bar{E}$, the values of L_d should be further increased. Moreover, the charge carriers migrate within clusters of Si crystallites, moving to the crystallites with minimum energy gaps. This also leads to a significant increase of the distances that electrons and holes travel in the thermalization process.

The excitation pulse is at least 10^4 times longer than τ_l. Thus, recombination is already efficient in the process of excitation. It can be concluded that at this stage most of the electron–hole pairs recombine non-radiatively. We did not observe an additional intense emission component during the UV laser pulse exposure, though for the excitation levels employed each of the Si crystallites contained at least several electron–hole pairs. If recombination was radiative this should have led to the existence of an intense PL component with time constants on a timescale below tens of nanoseconds. Most of the PL quanta were emitted after the end of the excitation pulse (see also section 3). For simplicity we will assume below that all non-equilibrium electron–hole pairs that exist in PS after the end of the excitation pulse recombine radiatively. This corresponds to 10^{18}–$10^{19}\ \mathrm{cm}^{-3}$ electron–hole pairs in the case of the PS specimens of section 3. Below, we will show that this assumption does not influence the results concerning PL kinetics significantly.

For the above-mentioned quantities of electron–hole pairs, some of the silicon crystallites are free of captured electrons or holes after the excitation pulse. Two principal scenarios of the recombination kinetics can be considered:

(a) In the case where the energy barriers between the clusters are high enough ($\Delta E < 0$), electrons and holes are thermalized in the same or the nearest potential wells. At first, the geminate pairs thermalized in one crystallite (or cluster of crystallites) recombine. In the next step we observe recombination of pairs that correspond to nearest crystallites. Pairs with larger separations still exist. We argue that this scenario is valid for oxidized porous silicon, and present corresponding experimental evidence in section 3. For as-prepared (red-orange-emission) specimens we could not explain the shapes of the PL spectra and the corresponding PL kinetics in terms of this mechanism alone, though we cannot rule out geminate recombination at least at the very beginning of the recombination process and also for crystallites with small ΔE values (blue crystallites).

(b) The other limiting situation that is consistent with our experimental results and that will be analysed in detail below is distant-pair recombination. As in [20, 21], we argue that non-equilibrium electrons and holes travel a certain distance before undergoing radiative recombination (figure 2). The rate of recombination due to tunnelling between crystallites with surfaces at a distance x is given by

$$\upsilon_1(x) = \tau_p^{-1}\mathrm{e}^{-2x/a} \tag{4}$$

where $\tau_p = 10^{-8}$ s†, and $a = 0.1$–0.2 nm for the case of the Si–SiO_2 barrier and 0.5–1 nm in the limiting case of Si:H barriers. As the value of a is very small, while the lifetime

† The high τ_p-values, compared with the standard 10^{-10} s, are due to large polarization effects in the surface region where the luminescent centres reside.

increases exponentially with separation, equation (4) predicts the existence of electron–hole pairs with lifetimes exceeding any reasonable experimental values. Therefore, we take into account an additional transport channel due to localized states in the disordered dielectric interconnecting Si crystallites. We consider that electrons and holes can diffuse the corresponding distances x by hopping between localized sites, as is shown by dashed curves in figure 2. The corresponding time constant can be written as

$$\tau_2 = \frac{x^2}{D_h} \tag{5}$$

where the diffusion coefficient of the hopping process can be written as

$$D_h = (1/6\tau_p)b^2 \exp(-W/kT)$$

where b is the distance between the localized states, and the activation energy of the hopping process W is of the order of a few tenths of an electron volt at room temperature and tends to zero for $T \to 0$. The above-mentioned diffusion process is also a downward hopping. We assume below that the energy loss in the process of transfer between neighbouring crystallites is always smaller than the difference of the corresponding band edges. This ensures that electrons and holes are thermalized in potential wells of silicon domains.

Our Monte Carlo simulation of the radiative recombination takes into account both types of electron and hole transfer. Once again we want to emphasize that this is in principle different from the Monte Carlo simulation performed in [24]. We create electrons and holes randomly at crystallites with different values of r_i and let them relax by downward hopping (direct tunnelling or diffusion) between the crystallites. Generation of electrons and holes in the Monte Carlo procedure can take place in any Si crystallite. In the case where an electron is generated in a crystallite of a cluster consisting of several particles, it moves to the Si particle with minimum E_g. This is a rapid process compared with the timescale of the radiative recombination. We also assume that electrons and holes that get into one crystallite or cluster of crystallites in the process of the initial distribution generation recombine non-radiatively before the onset of the radiative recombination. They do not influence the number of pairs that exist at the beginning of the light emission. As for the distant electron–hole pairs, we consider that a quantum of light with the wavelength given by equation (1) is emitted as soon as they meet in the crystallite r_i in the process of downward hopping. Backward activation hops of electrons with a probability proportional to $\exp((\Delta E_{gi} - \Delta E_{gj})/2kT)$ are also taken into account in the simulation. A possibility exists that some of the electrons or holes will experience hops, there and back, between neighbouring crystallites that are equal in size. In this case, after the first hop between equal domains, electrons and holes are directed to the nearest Si particle that is larger in size. As time passes, electrons and holes, most of which were trapped in small crystallites, travel to deeper energy states (large crystallites). Therefore a peak in the PL spectra corresponds to intermediate values of wavelengths. There is an optimal value of r_i for which electrons and holes have already found each other and their concentration is still high (see also the discussion in section 4). In the process of the simulation, electron–hole pairs were allowed to recombine until their density decreased to 30% of its initial value. The process was repeated ten times for a certain space configuration, then the configuration was changed. The results were averaged over all 150 configurations. Temporal dependencies of the quantities for the emitted quanta were obtained for different wavelengths (values of r_i). Figures 3(a), 3(b) show results illustrating the fate of ten electron–hole pairs that recombine radiatively at 300 K and 15 K respectively.

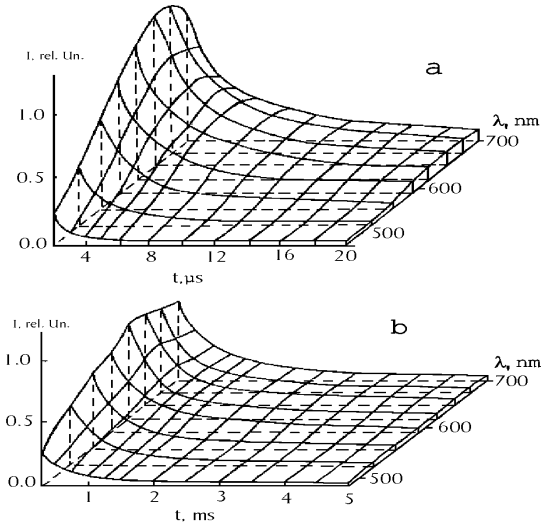

Figure 3. Calculated PL intensities as functions of time for different emission wavelengths: (a) $T = 300$ K; (b) $T = 15$ K.

The parameters of the crystallite size Gaussian distribution and the values of the diffusion coefficients D_h at room and helium temperatures were the only parameters that strongly influenced the final results. They were selected so as to obtain the best fits of the experimental data for porous silicon PL spectra in section 3, and are given in table 1. The value of D_h at $T = 300$ K can be obtained from equation (5) for the reasonable parameters $b = 1$ nm and $\Delta E = 0.1$ eV.

Table 1. The parameters of the crystallite size Gaussian distribution and the values of the diffusion coefficients D_h at room and helium temperatures.

Parameters	Values
Mean radius r of Si crystallites	0.7 nm
Dispersion of crystallite sizes, δ	1 nm
Pre-exponential factor in the Gaussian distribution	500
Tunnelling constant, a	0.15 nm
Phonon frequency, τ_p^{-1}	10^8 s^{-1}
Diffusion coefficient, D_{hv}, at 300 K	2×10^{-9} cm^2 s^{-1}
Diffusion coefficient, D_{hv}, at 15 K	2×10^{-11} cm^2 s^{-1}
Number of electron–hole pairs in one configuration	850

We stress that the results shown in figure 3 are rather insensitive to the value of the initial electron–hole density N_i. Variations of N_i in the range from 100 to 1500 pairs in the cube selected for simulation did not result in significant changes of the averaged $I(\lambda)$ dependencies. We attribute this fact to the existence of 'favourite' recombination paths for electron–hole pairs. These mesoscopic mechanisms of charge transport between the Si crystallites lead to the peculiarities of the $I(t, \lambda)$ dependencies for a certain configuration. These dependencies for one space configuration and two wavelengths are shown in figure 4. For each type of crystallite (with λ_1 and λ_2) there exist favourite transport paths with certain time constants. A large number of non-equilibrium charge carriers generated in PS recombine along 'favourite' paths. It is clear that this effect will be more pronounced for smaller arrays of Si particles.

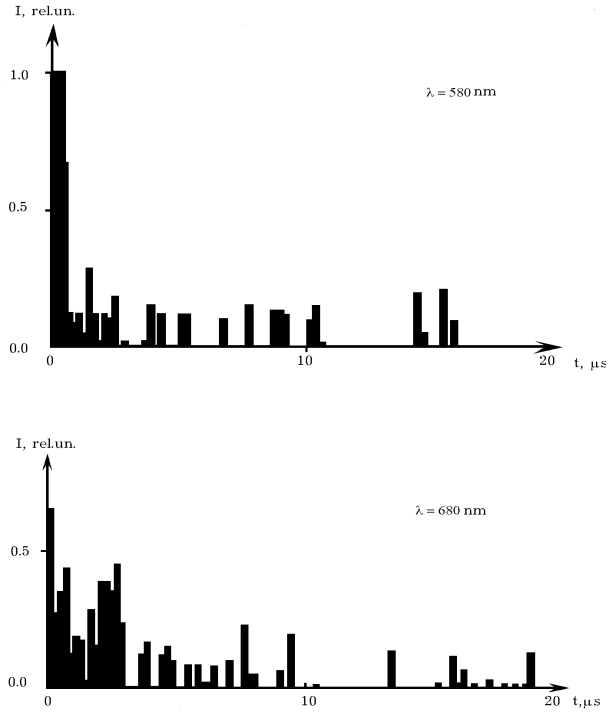

Figure 4. Time dependencies of the PL intensity for a single spatial configuration.

We have also performed an attempt to simulate the fate of geminate electron–hole pairs trapped in neighbouring crystallites. We were unable to explain the spectral and temporal dependencies of PL luminescence on nanosecond–millisecond timescales by geminate recombination. Nevertheless, we argue that this process is the cause of PS phosphorescence and can also contribute at the beginning of the PL decay process. Intense phosphorescence of PS was observed for the first time in this work, and will be discussed in sections 3 and 4.

3. Measurements of PS photoluminescence

3.1. Experimental procedure

Porous Si films were prepared from boron-doped p-type (1 Ω cm) silicon wafers. Electrochemical etching was performed in 15% HF/ethanol (volume ratio 1:2) electrolyte at current densities of 20–40 mA cm^{-2}. The anodization time ranged from 60 to 90 min. The films obtained had thicknesses of about 10 mm. Specimens obtained at current densities in the range 30–40 mA cm^{-2} showed the typical orange-red-colour PL. Specimens obtained at current densities exceeding 40 mA cm^{-2} emitted blue light. Specimens oxidized at 500–600 °C in the open air had properties similar to those of specimens obtained at high current densities. Pulsed nitrogen lasers ($\tau_p = 10$ ns, $\lambda = 337$ nm, 20 mJ/pulse; and $\tau_p = 5$ ns, $\lambda = 337$ nm, 10 mJ/pulse) were used as PL excitation sources. The power density in a single pulse ranged from 3×10^4 to 3×10^9 W cm^{-2}.

Quasistationary PL spectra were measured using a photon-counting system consisting of a monochromator, a Stanford Research 400 counter, and a PC. The PL signal was registered

using a photomultiplier and then directed to the multichannel analyser (NTA-1024EMG). The set-up also allowed us to set delay times in the range from 10 ns to 1 s between the excitation pulse and the beginning of the registration of the emitted quanta. This regime was used, in particular, for measurements of the PS phosphorescence.

In another version of the PL spectral measurements the ac signal at the repetition frequency of the UV laser was measured by a lock-in nanovoltmeter. In the microsecond range we also used a high-speed oscilloscope (the time constant of the registration circuit was about 100 ns) to display the PL decay kinetics. Temperature dependencies of the emission spectra and lifetimes were measured in the 15 K–300 K range using a Spectrum (CTI) helium microcooler equipped with an Oxford Instruments controller. Investigations at room temperatures were performed in the open air. The measurements of the emitted light polarization were made using precision polarizers and analysers. The spectral dependencies of the degree of polarization were obtained using a set of bandpass optical filters. A special chamber was designed to eliminate the effects of stray excitation light penetration to the entrance of the quanta registration system.

3.2. Spectral and temporal dependencies of the PL

Figure 5 shows the results of time-resolved luminescence measurements for an as-etched (30 mA cm^{-2}) PS sample at 15 K (curve (a)) and room temperature (curve (b)). Taking into account the fact that the PL decay is not exponential, following [19] we infer that the characteristic decay time

$$\tau_e = I_0^{-1} \int_0^\infty I(t)\,\mathrm{d}t. \tag{6}$$

The values of τ_e depend upon the wavelength and tend to saturate in the infrared spectral region. The energy of the PL spectral peak decreases in the process of PL decay. The decay curves become steeper. The shapes of the $I(t, \lambda)$ spectra did not change significantly for different excitation rates. The value of I depended linearly on the excitation power, with a tendency to saturation for powers of UV pulses exceeding 10^8 W cm^{-2}. Figure 6 shows the dependence of τ_e on temperature. Unlike the authors of [19], we did not observe saturation of τ_e below 50 K. At 15 K the values of τ_e are increased by approximately two orders of magnitude compared with those at room temperature. Figure 7 shows $I_i(\lambda)$ dependencies integrated over time at

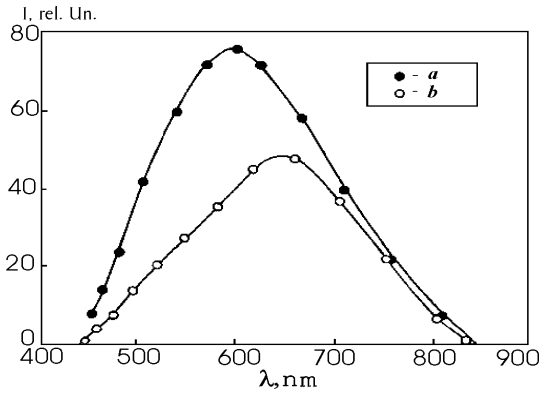

Figure 5. Time-resolved photoluminescence of porous silicon at different wavelengths for $T = 15$ K (curve (a)) and $T = 300$ K (curve (b)). (An as-prepared PS specimen with red-orange-colour light emission.)

room temperature and at 15 K. The spectral peak shifts 50 nm towards the direction of shorter wavelengths when T is lowered from 300 K to 15 K. The absolute value of I_i at 15 K increases only 1.5 times. Thus, the number of quanta emitted at room temperature when the decay times are tens of microseconds and at 15 K when the decay times are milliseconds are of the same order.

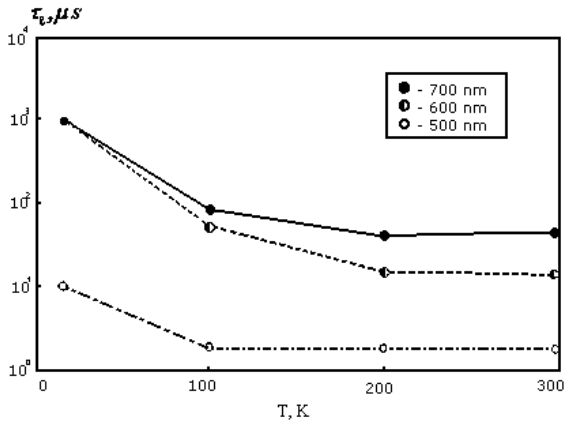

Figure 6. Dependencies of the effective PL lifetime τ_e on temperature for different emission wavelengths.

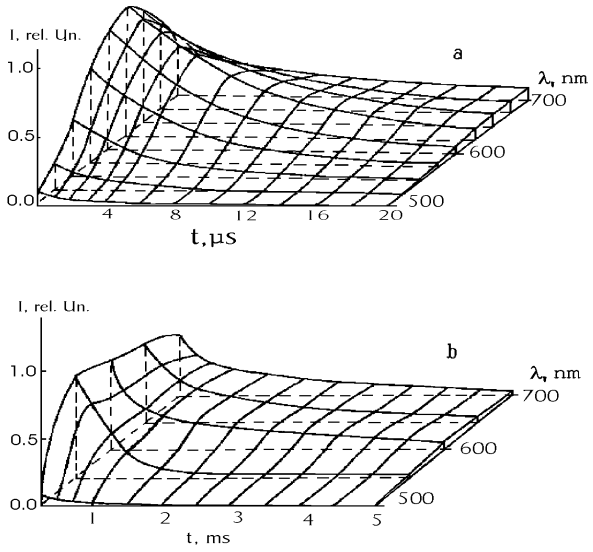

Figure 7. PL spectra (integrated over time) for the as-prepared PS sample at $T = 300$ K (a) and $T = 15$ K (b).

The most distinguishing feature of PL at 15 K is that in addition to millisecond decay we observed phosphorescence on a scale of seconds. This long-lasting emission was seen with the naked eye and was characterized by time constants of the order of 0.5 s. Figure 8 (curve (a)) shows the spectral dependence of the phosphorescence measured by integration, setting a delay

equal to 0.1 s in the box-counting registration system. No detectable changes of the emission colour were observed in the process of the subsequent phosphorescence intensity decay. It is seen that the spectral peak of the phosphorescence is shifted by about 50 nm towards the blue spectral region compared with the spectral peak at the end of the millisecond decay process. The phosphorescence disappeared when the temperature of the specimen was increased above 50 K.

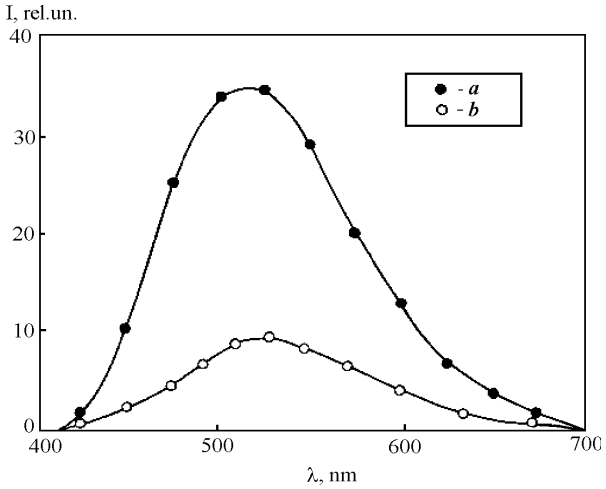

Figure 8. Phosphorescence spectra: curve (a): an as-prepared specimen at 15 K; curve (b): an oxidized specimen at 300 K.

We have also registered long-lasting blue-green emission of oxidized specimens (figure 8, curve (b)) at room temperature. This type of emission was about an order of magnitude weaker compared with the green phosphorescence at 15 K. The integral intensity increased less than twice when the temperature was lowered to 15 K and was also characterized by time constants of the order of 0.5 s. Similar results were obtained in our previous measurements of silica porous glasses with silicon impregnations [37, 38]. It should be noted that the blue phosphorescence was critically sensitive to the oxidation regime (oxidation time and temperature). The most pronounced effect was obtained for $T = 600\ ^{\circ}$C and $t = 180$ s.

In addition to the long-lasting component, PL with very small values of τ_e was registered. This type of PL decay was reported by a number of authors [16, 29, 39] and in our case was especially pronounced for 'oxidized' and 'partly oxidized' specimens. Spectral dependencies of the PL for samples annealed in the open air for different times (these and other PL spectra in this work were not corrected for the apparatus response) are shown in figure 9(a). It is evident that the shoulder at 400–500 nm of plot 1 (which corresponds to the as-prepared specimen) increases as a function of the oxidation time while the maximum at 630 nm decreases and shifts to the red. At the same time, the values of $\tau_e(\lambda)$ also undergo changes, as follows from figure 9(b). For the 'oxidized' specimens, they become comparable with the time constant of the registration system. The increase in the amount of oxygen resulting from 'oxidation' was confirmed by infrared transmission measurements (using an SF-29 spectrophotometer). The 910 nm peak typical for Si–O–Si bonds increased as a result of 'oxidation'. We want to emphasize that for short oxidation times of the order of tens of seconds, passivation of traps in the intercluster barriers is more probable than oxide thickness increase at the surfaces of crystallites. Therefore we put the term 'oxidation' in inverted commas.

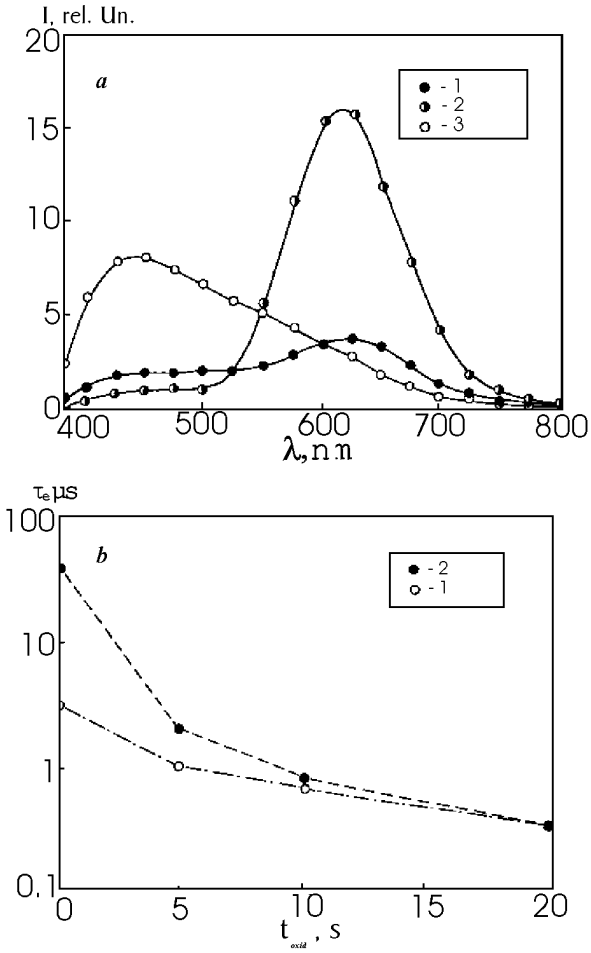

Figure 9. Changes of the PL for samples subjected to oxidation at $T = 500\ ^{\circ}$C: (a) PL spectra for different oxidation times: 1: 10 s oxidation; 2: initial; and 3: 1 min oxidation. (b) Dependencies of τ_e on the oxidation time for different wavelengths: 1: 550 nm, and 2: 650 nm.

3.3. Photoluminescence polarization

The emitted light showed a certain degree of linear polarization that was the same as the polarization of the incident exciting UV laser beam. The degree of polarization is defined as $D = (T_1 - T_2)/(T_1 + T_2)$, where T_1 and T_2 are the intensities of the PL components parallel and orthogonal to the polarization of the exciting light averaged over time. The degree of polarization reached, for our samples, a value of 10%. D was maximal for oxidized specimens at long wavelengths. The value of D was not dependent upon the direction of the exciting laser beam. Shown in figure 10 are the dependencies of D on λ for the as-prepared and oxidized samples. For the fresh specimens (red-orange emission) D first increased and then decreased monotonically with the increase of λ. The degree of polarization decreased with time for $\lambda > 500$ nm. The relaxation time was of the order of the PL decay time. Similar results were reported by other authors [40]. In the case of oxidized specimens, $D(\lambda)$ increased monotonically throughout the whole range of wavelengths. The same type of behaviour was

observed for specimens fabricated at large anodization currents. As was mentioned above, the decay times of the PL for these 'blue' samples were of the order of tens of nanoseconds. We were unable to perform time-resolved D-measurements due to limitations connected with the time constants of our equipment. We can only claim that blue emission with small lifetimes was strongly polarized.

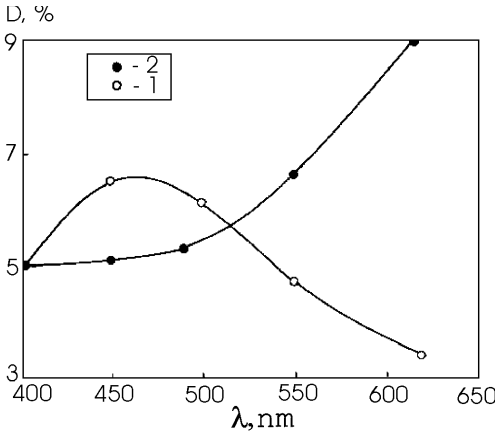

Figure 10. Dependencies of the degree of PL polarization D on wavelength for the as-prepared (1) and oxidized (2) specimens.

4. Discussion

As has already been mentioned, there is a very good agreement between the time-resolved PL spectra measured at 15 K and at room temperature and the results of the Monte Carlo simulation presented in section 2. This simulation was performed with the minimum number of fitting parameters. The parameters that give the best fits have reasonable values, typical for disordered solid-state systems. The problem solved corresponds to the case of distant-pair recombination in PS. The necessary intermixing of electrons and holes prior to radiative recombination was ensured by the high penetrability of the intercrystallite barriers. Our model also predicts the observed experimental dependence of τ_e on temperature. This relation is associated with the temperature dependence of the effective diffusion coefficient that determines the rate of hopping between Si crystallites and clusters of crystallites.

In the case of oxidized or partly oxidized PS, it is evident that the interconnection of crystallites is infringed. Non-stoichiometric SiO_x in the intercrystallite space can also be transformed into SiO_2. This leads to two main consequences:

(a) Electron–hole pairs are now thermalized mainly in the same cluster in which they were produced by the exciting quanta. Some of them travel very short distances and get into neighbouring crystallites.
(b) The hopping path between crystallites disappears due to the decrease of the hopping site concentration.

As a result, it is mostly geminate pairs that remain in PS after the end of the UV exciting pulse. It is clear that we can also meet an intermediate situation for partly oxidized samples. Geminate pairs that have thermalized in a single cluster give rise to PL characterized by very short lifetimes (curve 2 in figure 9(a)). The transformation of the luminescence from red to blue

is easily understood within this model. The process of oxidation is a kind of threshold-type process from the point of view of charge transport (the probabilities of charge transfer depend exponentially on the intercrystallite barrier parameters). The system can be considered as a mixture of 'oxidized' and initial porous silicon at intermediate stages of oxidation. For this intermediate situation, long-time 'favourite' paths are blocked, thus resulting in the decrease of τ_e. It is natural that the emission peak at 630 nm decreases drastically. The fact that a short-lifetime emission is observed in the long-wavelength wing of curve 2 in figure 9(a) means that geminate pairs now recombine in corresponding crystallites. A certain number of geminate electron–hole pairs existed in the as-prepared samples. This explains the short-wavelength shoulder (curve 1 in figure 9(a)) that is further transformed into the 'blue' peak for the 'oxidized' sample (curve 3 in figure 9(a)).

Recombination of geminate electrons and holes captured after thermalization in neighbouring Si domains leads to long-lasting emission. Only tunnelling (and not diffusion) between corresponding crystallites or clusters needs to be considered in this case. Thus time constants of the order of 0.5 s correspond to SiO_2 barriers with widths of about 1–1.8 nm (equation (4)). This is in accordance with the simulated spatial structure of PS. The corresponding PL spectra must be of the same shape for short-lived and long-lasting blue emissions. This is consistent with the experimental results of figure 8 (curve (a)) and figures 9(a) and 9(b). In the case where oxidation takes too long, the distances between Si fragments increase and the smallest of them are completely oxidized. This explains the high sensitivity of the effect to the oxidation regimes. We were able to find a fairly narrow parameter window for the fabrication of phosphorescent samples.

As was already mentioned, a certain number of geminate pairs can be present in 'red-orange' PS. The r-values for these pairs are $<\bar{r}$, where $\bar{r}$ is the mean distance between electrons and holes. The existence of geminate pairs explains the red-shift of the emission peak with the increase of τ_e registered in our experiments (figure 7) and the absence of observable rise times for the luminescence [31] (on scales of nanoseconds and microseconds). At elevated temperatures, geminate pairs can be separated by diffusion (hopping) processes. After separation, corresponding electrons and holes are indistinguishable from other non-equilibrium charge carriers. At low temperatures, when diffusion processes are suppressed, recombination of geminate pairs will determine the long-time emission processes. We argue that this is a plausible explanation of the observed green phosphorescence. The observed shift of the PL spectra measured with 0.1 s delays after the end of the exciting pulse also confirms this assumption. From the point of view of the model developed, this shift is evidence that electrons and holes emitted at $t > 0.5$ s did not participate in the diffusion processes in PS prior to recombination.

The spectral dependencies of the degree of PL polarization give additional evidence of the validity of the models proposed. The polarization of the light emitted from PS is explained by the existence of elongated Si domains [41, 42]. The absorption of light is more efficient when the direction of the E-vector of the exciting wave is parallel to the main axis of the elongated domains (e.g., due to polarization effects). From this point of view the increase of the degree of polarization D for both as-prepared and oxidized specimens in the violet spectral region (figure 10) can be attributed to the increase of the numbers of probated Si clusters that emit in this spectral range. In the case of oxidized PS, when diffusion processes are suppressed, a monotonic increase of D is observed. For as-prepared (red-orange) PS, the value of D decreases when diffusion processes dominate. The dominance of distant-pair recombination also explains the decay of D in time-resolved polarization measurements. The corresponding decay times of D are of the same order as τ_e, because electrons and holes of those geminate pairs that dissociate use the same transport paths as the charge carriers thermalized at random.

5. Conclusions

The experimental results presented in this paper give evidence that the range of photoluminescence lifetimes in porous silicon should be extended at least to τ_e of the order of seconds. This strongly implies that tunnelling processes must be taken into account in attempts to interpret the whole range of time constants on single premises. The model presented in this paper provides a satisfactory understanding of most aspects of radiative recombination in PS, including the spectral and temporal dependencies of the PL and the peculiarities of the degree of polarization of the emitted light. It also gives an adequate explanation of the phosphorescence revealed in PS. We have shown that both geminate and distant-pair recombination processes take place in PS, and that at room temperature distant-pair recombination dominates at least after a certain time delay after the end of the exciting UV laser pulse. We have performed a direct Monte Carlo simulation of the distant-pair recombination. Our model, which starts with few, and very general, assumptions, differs from analogous models for amorphous semiconductors in the existence of a certain disordered PS structure that was also modelled by a separate Monte Carlo procedure. It also differs from the existing Monte Carlo simulations of PS by taking into account both electron and hole hopping below the mobility edges. We have also assumed the existence of an additional hopping path for electrons and holes travelling between silicon domains. With reasonable values of a small number of fitting parameters, we obtained good agreement between the calculations and the $I(\lambda, t)$ dependencies at room and helium temperatures.

The proposed radiative recombination model takes into account both nanosized domains in PS and traps in the media between these domains. Thus, our model predicts strong changes of the PS photoluminescence as a result of various chemical and thermal treatments. But in contrast to the case for other research [10], the traps mentioned act as transport sites in diffusion processes. We do not claim that we provide support for a certain model of the final microscopic process of radiative recombination in PS. In particular, both recombinations of excitons confined in quantum dots and recombination at the surfaces of quantum crystallites can be considered as plausible options that do not contradict our model. However, the results obtained give evidence that quantum confinement in silicon domains and charge transport between these domains must be taken into account in any interpretation.

Direct confirmation of electron and hole migration prior to recombination could be obtained from time-resolved spectral measurements of the PL from areas as small as a few tenths of a square micrometre. In this case, mesoscopic effects connected with the existence of 'favourite' transport paths (figure 3) should become pronounced, and would result in individual peculiarities on the decay curves. Unfortunately, at present the sensitivity of our equipment is insufficient for us to perform these measurements.

Acknowledgments

This work was partially funded by the Civilian Research Development Foundation (CRDF) through Grant No UP1-368 and by the Ukrainian–Israeli joint scientific project through Grant No 2M/1807-97.

References

[1] Canham L T 1990 *Appl. Phys. Lett.* **57** 1046
[2] Cullis A G and Canham L T 1991 *Nature* **353** 335
[3] Lehmann V and Gosele U 1991 *Appl. Phys. Lett.* **58** 856

[4] Gardelis S, Rimmer I S, Dawson P, Halimaoui B, Kubialc R A, Whall T E and Parker E H C 1991 *Appl. Phys. Lett.* **59** 2113
[5] Lin C H, Lee Si C and Chen Y F 1993 *Appl. Phys. Lett.* **63** 902
[6] Behrensmeier R, Namavar F, Amisela G B, Otter F A and Galligan I M 1993 *Appl. Phys. Lett.* **62** 2408
[7] Prokes S M, Glembocki O I, Bermudez V M, Kaplan R, Friedersdart L E and Searson P C 1992 *Phys. Rev.* B **45** 13 788
[8] Braudl M S, Fuchs H D, Stutzmann M, Weber S and Cardona M 1992 *Solid State Commun.* **81** 307
[9] Tsai C, Li K H, Kinosky P S, Qian R Z, Hau T C, Irby I T, Banejee S K, Hause B K and White I M 1992 *Appl. Phys. Lett.* **60** 1700
[10] Lockwood D J 1994 *Solid State Commun.* **92** 101
[11] Kanemitsu Y, Uto H, Masumoto Y, Matsumoto T, Fukagi T and Mimura H 1993 *Phys. Rev.* B **48** 2827
[12] Dumas D, Gu M, Sysykh C, Gimzewsky I K, Makarenko T, Halimaoui A and Salvan F 1993 *Europhys. Lett.* **23** 197
[13] Koch F 1993 *MRS Proc.* **298** 319
[14] Koch F, Petrova-Koch V and Muschik T 1993 *J. Lumin.* **57** 271
[15] Qin G G and Iia Y Q 1993 *Solid State Commun.* **86** 559
[16] Tsybeskov L, Vandyshev Yu V and Fauchet P M 1994 *Phys. Rev.* B **49** 7821
[17] Matsumoto T, Daimon M, Futagi T and Mimura H 1992 *Japan. J. Appl. Phys.* **31** L619
[18] Takazawa A, Tamura T and Yamada M 1993 *Appl. Phys. Lett.* **63** 940
[19] Xie Y H, Hybertsen M S, Wilson W L, Ipri S A, Carver G E, Brown W L, Dons E, Weir B E, Kortan A R, Watson G P and Liddle A I 1994 *Phys. Rev.* B **49** 5386
[20] Dunstan D I and Boulitrop F 1984 *Phys. Rev.* B **30** 5945
[21] Levin E I, Marianer S, Shklovskii B I and Fritzsche H 1991 *J. Non-Cryst. Solids* **137** 559
[22] Gutschker O and Binderman R 1991 *J. Non-Cryst. Solids* **137** 579
[23] Ventura P J, do Carmo M C and O'Donnell K P 1995 *J. Appl. Phys.* **77** 323
[24] Pavesi L and Roman E H 1995 *MRS Proc.* **358** 549
[25] Takagahara T and Takeda K 1992 *Phys. Rev.* B **46** 15 578
[26] Shik A 1993 *J. Appl. Phys.* **74** 2951
[27] Suemoto T and Tanaka T 1994 *Phys. Rev.* B **49** 11 005
[28] Vial I C, Bsiesy A, Gaspard F, Herino R, Ligeon M, Muller R, Romestain R and Macfarlane R M 1992 *Phys. Rev.* B **45** 14 171
[29] Kanemitsu Y, Futagi T, Matsumoto T and Mimura H 1993 *Phys. Rev.* B **49** 14 732
[30] Proces S M 1993 *Appl. Phys. Lett.* **65** 3244
[31] Laiho R, Pavlov A, Novi O and Tsuboi T 1993 *Appl. Phys. Lett.* **63** 275
[32] Mihalcescu I, Vial J C and Romestain R 1996 *J. Appl. Phys.* **80** 2404
[33] Tsybeskov L, Peng C, Duttagupta S P, Ettedgui E, Gao V, Fauchet P M and Curver G E 1993 *Proc. MRS* **298** 307
[34] Landau L D and Lifshitz E M 1972 *Quantum Mechanics* (Moscow: Nauka) p 114
[35] Sanders G D and Chaus Y C 1992 *Phys. Rev.* B **45** 9202
[36] Proot I R, Delerue C and Allen G 1992 *Appl. Phys. Lett.* **61** 1948
[37] Roizin Ya O, Korlakov A B and Gevelyuk S A 1994 *MRS Proc.* 346
[38] Roizin Ya O, Alexeev-Popov A V, Gevelyuk S A, Savin D P, Mugenski E and Sokolska I 1996 *J. Phys. Chem. Glasses* **11** 68
[39] Morisaki N, Nashimoto N, Ping F W, Nozawa N and Ono H 1993 *J. Appl. Phys.* **74** 2977
[40] Andrianov A V, Kovalev D I, Zinoviev N N and Yaroshetskii I D 1993 *JETP Lett.* **58** 428
[41] Xie Y N, Wilson W L, Koss F M, Mucha I A, Fitzgerald E A, Macaulay I M and Harris T D 1992 *J. Appl. Phys.* **75** 2403
[42] Suris R A and Lavallard P 1995 *Solid State Commun.* **95** 267